

# 1 **Role of slope on infiltration: a review**

2

3 Renato Morbidelli<sup>1</sup>, Carla Saltalippi, Alessia Flammini

4 Dept. of Civil and Environmental Engineering, University of Perugia, via G. Duranti 93, 06125 Perugia, Italy

5

6 Rao S. Govindaraju

7 Lyles School of Civil Engineering, Purdue University, West Lafayette, IN 47907

8

9

## 10 **Abstract**

11 Partitioning of rainfall at the soil-atmosphere interface is important for both surface and  
12 subsurface hydrology, and influences many events of major hydrologic interest such as  
13 runoff generation, aquifer recharge, and transport of pollutants in surface waters as well as the  
14 vadose zone. This partitioning is achieved through the process of infiltration that has been  
15 widely investigated at the local scale, and more recently also at the field scale, by models that  
16 were designed for horizontal surfaces. However, infiltration, overland flows, and deep flows  
17 in most real situations are generated by rainfall over sloping surfaces that bring in additional  
18 effects. Therefore, existing models for local infiltration into homogeneous and layered soils  
19 and those as for field-scale infiltration, have to be adapted to account for the effects of surface  
20 slope. Various studies have investigated the role of surface slope on infiltration based on a  
21 theoretical formulations for the dynamics of infiltration, extensions of the Green-Ampt  
22 approach, and from laboratory and field experiments. However, conflicting results have been  
23 reported in the scientific literature on the role of surface slope on infiltration. We summarize  
24 the salient points from previous studies and provide plausible reasons for discrepancies in  
25 conclusions of previous authors, thus leading to a critical assessment of the current state of

---

<sup>1</sup> Correspondence to: R. Morbidelli, Department of Civil and Environmental Engineering, University of Perugia, Via Duranti 93, 06125 Perugia, Italy. E-mail: [renato.morbidelli@unipg.it](mailto:renato.morbidelli@unipg.it)

26 our understanding on this subject. We offer suggestions for future efforts to advance our  
27 knowledge of infiltration over sloping surfaces.

28

29 **KEYWORDS** Hillslope hydrology, overland flow, infiltration process, infiltration modeling

30

31

32

### 33 **1. Introduction**

34 The process of infiltration is controlled by many factors, including soil depth and  
35 geomorphology, soil hydraulic properties, and rainfall or climatic properties. The spatio-  
36 temporal evolution of infiltration rates under natural conditions cannot be currently deduced  
37 by direct measurements alone at any scale of interest in applied hydrology, therefore the use  
38 of infiltration models that rely on measurable quantities is of fundamental importance.

39 Even though the representation of the natural processes of areal infiltration over both flat and  
40 sloping surfaces is needed in hydrologic models, research activity has been limited to the  
41 development of local, or point, infiltration models for many years. A variety of local  
42 infiltration models for vertically homogeneous soils with constant initial soil water content  
43 and over horizontal surfaces have been proposed (Green and Ampt, 1911; Kostiakov, 1932;  
44 Horton, 1940; Holtan, 1961; Swartzendruber, 1987; Philip, 1957a,b,c; Soil Conservation  
45 Service, 1972; Smith and Parlange, 1978; Broadbridge and White, 1988; Dagan and Bresler,  
46 1983; Corradini et al., 1994). Furthermore, for isolated storms and when ponding is not  
47 achieved instantly, extended forms of the Philip model (Chow et al., 1988), Green-Ampt  
48 model (Mein and Larson, 1973; Chu, 1978) and the Smith and Parlange model (Parlange et  
49 al., 1982) are widely used. However, for complex rainfall patterns involving rainfall hiatus  
50 periods or a rainfall rate after time to ponding less than soil infiltration capacity, these models  
51 are not directly applicable because the assumption of uniform initial soil moisture cannot be  
52 met for successive storms. Alternatively, an approach for the application of the

53    aforementioned classical models was developed (MIs, 1980; Péschke and Kutílek, 1982; and  
54    Verma, 1982) starting from the time compression approximation proposed by Reeves and  
55    Miller (1975) for post-hiatus rainfall producing immediate ponding. However, Smith et al.  
56    (1993) by comparison with results of the Richards equation showed that the last approach was  
57    not sufficiently accurate because it neglects the soil water redistribution process which is  
58    particularly important when long periods with a light rainfall or a rainfall hiatus occur. A  
59    more general model that combines infiltration and redistribution was provided by Corradini et  
60    al. (1997) starting from the Darcy and continuity equations then combined with a conceptual  
61    representation of the wetting soil moisture profile.

62    Natural soils are rarely vertically homogeneous. In hydrological simulations, the estimate of  
63    effective rainfall can be reasonably schematized by a two-layered vertical profile (Mualem et  
64    al., 1993; Taha et al., 1997). A general semi-analytical/conceptual model for crusted soils was  
65    formulated by Smith et al. (1999), and was extended by Corradini et al. (2000) to represent  
66    infiltration and re-infiltration after a redistribution period under any rainfall pattern and for any  
67    two-layered soil where either layer may be more or less permeable than the other. For a much  
68    more permeable upper layer, and under more restrictive rainfall patterns, a simpler semi-  
69    empirical/conceptual model was presented by Corradini et al. (2011). Under conditions of  
70    surface saturation, a simple Green-Ampt based model was proposed (Chow et al., 1988).

71    In applied hydrology, upscaling of point infiltration modeling to the field scale is required to  
72    estimate the areal-average infiltration. This is a complex task because of the natural spatial  
73    heterogeneity of hydraulic soil properties (Nielsen et al., 1973; Warrick and Nielsen, 1980;  
74    Greminger et al., 1985; Sharma et al., 1987; Loague and Gander, 1990) and particularly of the  
75    soil saturated hydraulic conductivity (Russo and Bresler, 1981; 1982) that may be assumed as  
76    a random field with a lognormal univariate probability distribution. Some models representing  
77    infiltration at the field scale have been proposed with saturated hydraulic conductivity,  $K_s$ ,

78 assumed as a random variable at the soil surface for both uniform (Smith and Goodrich, 2000;  
79 Govindaraju et al., 2001) and non-uniform soils (Corradini et al., 2011; Govindaraju et al.,  
80 2012) in the vertical direction. Further, models were developed to describe the effects of a  
81 joint horizontal variability of  $K_s$  and rainfall rate  $r$  (Wood et al., 1986; Castelli, 1996;  
82 Govindaraju et al., 2006; Morbidelli et al., 2006), and of the spatial variability of initial soil  
83 moisture content  $\theta_i$  (Smith and Goodrich, 2000). The role of the heterogeneity of  $\theta_i$ , combined  
84 with uniform values of  $K_s$  and  $r$  or with  $K_s$  randomly variable, has been widely analyzed for  
85 different spatial scales (Brontsert and Bardossy, 1999; Morbidelli et al., 2012; Hu et al.,  
86 2015).

87 Most of the above-mentioned models consider a horizontal soil surface or one with a low  
88 slope that does not affect the infiltration process. However, in most real situations infiltration  
89 occurs in surfaces characterized by different gradients (Beven, 2002; Fiori et al., 2007) and  
90 the role of surface slope on infiltration is not clear. In fact, the results obtained by some  
91 theoretical (Philip, 1991; Chen and Young, 2006; Wang et al., 2018) and experimental  
92 investigations (Nassif and Wilson, 1975; Sharma et al., 1983; Poesen, 1984; Cerdà and  
93 García-Fayos, 1997; Fox et al., 1997; Chaplot and Le Bissonnais, 2000; Janeau et al., 2003;  
94 Assouline and Ben-Hur, 2006; Essig et al., 2009; Ribolzi et al., 2011; Patin et al., 2012; Lv et  
95 al., 2013; Morbidelli et al., 2015; Mu et al., 2015; Khan et al., 2016; Morbidelli et al., 2016)  
96 lead to rather contrasting conclusions, suggesting an improved understanding and modeling of  
97 infiltration over sloping surfaces is required.

98 The overall intent of this paper is to highlight the state of the art on the slope-infiltration  
99 relationship and provide guidance for future developments on the basis of available results.

100

101

102

103

## 104 **2. Theoretical Formulations**

105

### 106 2.1 Analytical formulation

107 Let consider a long planar hillslope consisting of a homogeneous isotropic soil, with slope  
108 angle  $\gamma$ , and Cartesian rectangular spatial coordinates  $x$  and  $z$ , with  $x$  and  $z$  positive in the  
109 horizontal downslope direction and in the downward vertical direction, respectively. Let  
110 introduce also the rotated coordinates  $(x^*, z^*)$ , as defined in Fig. 1, for explicitly accounting  
111 for slope:

112

$$113 \quad x^* = x \cos(\gamma) + z \sin(\gamma) \quad (1)$$

$$114 \quad z^* = -x \sin(\gamma) + z \cos(\gamma) \quad (2)$$

115

116

117 *insert here Fig. 1*

118

119

120 According to Philip (1957b; 1969) the equation that governs unsaturated soil water movement  
121 may be expressed in the form:

122

$$123 \quad \frac{\partial \theta}{\partial t} = \nabla \cdot (D \nabla \theta) - \frac{dK}{d\theta} \frac{\partial \theta}{\partial z} \quad (3)$$

124

125 with  $t$  the time,  $\theta$  the volumetric soil water content,  $D$  the soil diffusivity, and  $K$  the hydraulic  
126 conductivity, being  $D$  and  $K$  typically nonlinear functions of  $\theta$ .

127 We first examine the dynamics of infiltration and downslope water transport by searching for  
 128 the solution of eq. (3) under the conditions:

129

$$130 \quad t=0 \quad z^*>0 \quad \theta=\theta_0 \quad (4)$$

$$131 \quad t>0 \quad z^*=0 \quad \theta=\theta_1 \quad (5)$$

132

133 where  $\theta_0$  is the uniform initial volumetric soil water content, and  $\theta_1$  is the value of  $\theta$   
 134 associated to the capillary head  $\psi_1$  at which water is available at the soil surface  $z^*=0$ . Under  
 135 the hypothesis of negligible depth of free water excess on the hillslope,  $\psi_1=0$  and  $\theta_1$  is the  
 136 saturated volumetric soil water content.

137 Expressing eq. (3) in terms of  $x^*$  and  $z^*$ , we derive:

138

$$139 \quad \frac{\partial \theta}{\partial t} = \nabla \cdot (D \nabla \theta) - \frac{dK}{d\theta} \left[ \frac{\partial \theta}{\partial x^*} \sin(\gamma) + \frac{\partial \theta}{\partial z^*} \cos(\gamma) \right] \quad (6)$$

140

141 Except for a small upper area of the hillslope, the relevant solution of eq. (6) subject to the  
 142 conditions of eqs. (4) and (5) is basically independent of  $x^*$  and depends only on  $z^*$  and  $t$ . On  
 143 this basis, we may rewrite eq. (6) as:

144

$$145 \quad \frac{\partial \theta}{\partial t} = \frac{\partial}{\partial z^*} \left[ D \frac{\partial \theta}{\partial z^*} \right] - \frac{dK}{d\theta} \frac{\partial \theta}{\partial z^*} \cos(\gamma) \quad (7)$$

146

147 We note that eq. (7) subject to eqs. (4) and (5) is formally identical to the classical one-  
 148 dimensional infiltration equation, if  $K$  is substituted by  $K \cos(\gamma)$ .

149 Reverting to the non-rotated axes  $x$  and  $z$ , eq. (7) becomes:

150

151 
$$\frac{\partial \theta}{\partial t} = \frac{\partial}{\partial z} \left[ D \frac{\partial \theta}{\partial z} \right] \sec^2(\gamma) - \frac{dK}{d\theta} \frac{\partial \theta}{\partial z} \quad (8)$$

152

153 The vertical component of the unsaturated water flux,  $v$ , may be expressed as:

154

155 
$$v = K - D \frac{\partial \theta}{\partial z} \quad (9)$$

156

157 while its value at the surface  $z=x \sin(\gamma)$ ,  $v_0$ , may be considered the infiltration rate of standard

158 hydrologic practice, provided by:

159

160 
$$v_0 = K_1 - \left( D \frac{\partial \theta}{\partial z} \right)_{z=x \sin(\gamma)} \quad (10)$$

161

162 where  $K_1$  stands for  $K(\theta_1)$ .

163 We can introduce analogous quantities in terms of rotated coordinates  $(x^*, z^*)$ , denoting with

164  $v_n$  the infiltration rate normal to the hillslope:

165

166 
$$v_n = K \cos(\gamma) - D \frac{\partial \theta}{\partial z^*} \quad (11)$$

167

168 and its value for  $z^*=0$ ,  $v_{n0}$ :

169

170 
$$v_{n0} = K_1 \cos(\gamma) - \left[ D \frac{\partial \theta}{\partial z^*} \right]_{z^*=0} \quad (12)$$

171

172 The theoretical approach above described states that the gravitational effect in the direction  
173 normal to the slope decreases by a factor  $\cos(\gamma)$  and entails a small reduction of the infiltration  
174 rate, while capillary forces are invariant.

175 Along these lines, Philip (1991) suggested an analytical series solution and two simplified  
176 relationships for different time intervals. In order to explicit the comparison with infiltration  
177 rate for a horizontal soil surface he proposed these ratios:

178

$$179 \quad \lim_{t \rightarrow 0} \frac{v_{n0}(\gamma)}{v_{n0}(0)} = 1 \quad (13)$$

$$180 \quad \lim_{t \rightarrow \infty} \frac{v_{n0}(\gamma)}{v_{n0}(0)} = \cos(\gamma) \quad (14)$$

181

182 At short times, when the capillary forces drive the process, the infiltration rate normal to the  
183 slope doesn't depend on the slope angle (see eq. 13). On the contrary, at very long times,  
184 when only gravitational forces play a role,  $v_{n0}$  reduces with  $\cos(\gamma)$ , being the gravity force  
185 only vertical.

186

## 187 2.2 Conceptual formulation

188 From eq. (7), it may be derived that except for the difference of coordinate system, the only  
189 change needed for describing infiltration over a sloping surface is to substitute  $K$  with  $K$   
190  $\cos(\gamma)$ , and only the component of the water flux normal to the soil surface is changed by  
191  $\cos(\gamma)$ . On the contrary, the downslope component of gravity does produce flow, but it does  
192 not modify the soil moisture profile along the normal direction on a planar slope because the  
193 flow field is independent of  $x^*$ . As a consequence, as an approximation, the Green-Ampt  
194 (GA) model can be rearranged including the same modification.



195 On the basis of Darcy's law, Chen and Young (2006) proposed a modified version of the GA  
 196 model for a sloping surface under ponded conditions as:

197

$$198 \quad v_n = K_e \frac{z_f^* \cos(\gamma) + s_f + H}{z_f^*} \quad (15)$$

199

200 with  $K_e$  the effective saturated hydraulic conductivity,  $z_f^*$  the depth of the wetting front along  
 201 the direction normal to the slope surface,  $s_f$  the wetting front capillary head,  $H$  the ponding  
 202 water head on the surface, and  $z_f^* \cos(\gamma)$  the gravitational head at the wetting front (see Fig.  
 203 2). Physically, each variable is considered to remain invariant along the downslope direction.

204

205

206 *insert here Fig. 2*

207

208

209 Being the ponding depth on a sloping surface usually small if compared to the wetting front  
 210 capillary head  $s_f$ , in their theoretical analysis Chen and Young (2006) treated it as a revision  
 211 to  $s_f$ . The cumulative infiltration depth in the normal direction,  $I_n$ , can be determined as:

212

$$213 \quad I_n = (\theta_s - \theta_i) z_f^* \quad (16)$$

214

215 Taking the derivative of  $I$  with respect to time and substituting into eq. (15) yields:

216

$$217 \quad \frac{dz_f^*}{dt} = \frac{K_e}{(\theta_s - \theta_i)} \frac{z_f^* \cos(\gamma) + s_f + H}{z_f^*} \quad (17)$$

218

219 By integration with respect to time eq. (17) provides:

220

$$221 \quad t = \frac{(\theta_s - \theta_i)}{K_e \cos(\gamma)} \left[ z_f^* - \frac{(s_f + H)}{\cos(\gamma)} \ln \frac{z_f^* \cos(\gamma) + s_f + H}{s_f + H} \right] \quad (18)$$

222

223 Substituting eq. (16) into eq. (18) yields the following simplified form:

224

$$225 \quad K_e t \cos(\gamma) = I_n - \frac{SM}{\cos(\gamma)} \ln \left[ 1 + \frac{I_n \cos(\gamma)}{SM} \right] \quad (19)$$

226

227 with  $S=s_f+H$  and  $M=\theta_s-\theta_i$ .

228 Equation (19), that is the key equation of the GA model, describes in an implicit way the

229 variation in time of cumulative infiltration depth. Chen and Young (2006) expanded the

230 second term of the right-hand side of eq. (19) with a Taylor series on  $I_n$  around point  $I_n=0$  and

231 keeping the first two terms in the series yielded:

232

$$233 \quad K_e t \approx \frac{1}{2} \frac{I_h^2 \cos^2(\gamma)}{SM} \quad (20)$$

234

235 with  $I_h=I_n/\cos(\gamma)$  the cumulative depth in the vertical direction. This solution is valid only for

236 small time according to the converging range of Taylor series. The variable  $I_h$  compares

237 infiltration on a slope to that on a horizontal surface, but with the same horizontal projection

238 lengths, as:

239

240 
$$\frac{I_h(\gamma)}{I_h(0)} = \frac{1}{\cos(\gamma)} \quad (21)$$

241

242 This implies that the sloping surface increases the infiltration at small  $t$  by a factor  $1/\cos(\gamma)$ .

243 For  $t \rightarrow \infty$ , or for high infiltration depths, eq. (19) can be approximated as:

244

245 
$$K_e t \approx I_h \quad (22)$$

246

247 which highlights that the slope effect reduces with time and vanishes at very long  $t$ .

248 Therefore, according to Chen and Young (2006), infiltration at small times is controlled by

249 capillary forces, which would be independent of slope angle in case of homogeneous and

250 isotropic soils. However, when the slope angle increases the slope length increases, and

251 consequently also the total infiltration volume increases. For long  $t$  (or large  $I_h$ ), the gravity

252 becomes the control mechanism, and the normal flux would be reduced by the factor  $\cos(\gamma)$ .

253 This effect cancels with increasing slope length, and the net slope effect essentially vanishes.

254 The results by Chen and Young (2006), obtained through a modified form of the GA model,

255 depend by the condition of identical slope horizontal projection lengths. In fact, despite

256 apparently in contrast to the above results by Philip (1991), the modified GA model was

257 compared to a solution of Richards' equation on a sloping surface and was shown to match

258 well.

259 Wang et al. (2018) proposed a new theoretical formulation involving the estimate of ponding

260 time and infiltration on hillslopes under both steady and unsteady rainfall conditions. The

261 infiltrability equation was developed by integration of Darcy's law for sloping surfaces and

262 incorporating the flux-concentration equation (Sivapalan and Milly, 1989) as:

263

$$t = \frac{1}{\cos^2(\gamma)} \int_{\theta_i}^{\theta_s} \frac{D(\theta)(\theta - \theta_i)}{(N - K_i)^2 F} \left[ \ln \frac{i_n - N \cos(\gamma)}{i_n - K_i \cos(\gamma)} + \frac{(N - K_i) \cos(\gamma)}{i_n - N \cos(\gamma)} \right] d\theta \quad (23)$$

where  $i_n$  is the infiltrability normal to the surface slope,  $t$  is time,  $F = (\theta - \theta_i) / (\theta_s - \theta_i)$  and  $N = K_i + (K(\theta) - K_i) / F$ . Equation (23) leads to a scaling relation between infiltration on sloping surfaces and horizontal surfaces: under ponding conditions the normal infiltration rate on a sloping surface reduces to that on horizontal surface scaled through a proportionality factor equal to  $\cos(\gamma)$ , by taking  $1/\cos^2(\gamma)$  times the time for the horizontal plane:

$$t(\gamma) = \frac{t(0)}{\cos^2(\gamma)} \quad (24)$$

where  $t(\gamma)$  and  $t(0)$  are the times for slope and horizontal plane, respectively, associated to the same value of infiltrability.

For time to ponding,  $t_p$ , Wang et al. (2018) proposed the following equation:

$$t_p = \frac{1}{\cos^2(\gamma)} \int_{\theta_i}^{\theta_s} \frac{D(\theta)(\theta - \theta_i)}{(r - K_i) [F(r - K_i) - (K(\theta) - K_i)]} d\theta \quad (25)$$

where  $r$  is a constant rainfall rate, and they found that the ponding time for hillslopes can be estimated from that of horizontal plane through eq. (24).

After ponding and under steady rainfall conditions, eq. (23) could be solved for temporal evolution of infiltration. Alternatively, in order to avoid the required computational effort, Wang et al. (2018) selected an explicit empirical relation that links the infiltration rate with time including the slope effect as:

287  $i_n = at^b + K_s \cos(\gamma)$  (26)

288

289 where a and b are parameters related to initial soil moisture content, soil type and rainfall  
290 intensity. A procedure to extend the approach to unsteady rainfall was also included. The  
291 proposed approach was validated by comparison with results obtained by Hydrus 1D and by  
292 the modified GA model for sloping surfaces (Chen and Young, 2006).

293

### 294 **3. Experimental Evidence**

295 Investigations to address the understanding of the effect of surface slope on the infiltration  
296 process have been performed through some experiments in both laboratory (Nassif and  
297 Wilson, 1975; Poesen, 1984; Fox, et al., 1997; Assouline and Ben-Hur, 2006; Essig et al.,  
298 2009; Lv et al., 2013; Morbidelli et al., 2015; Mu et al., 2015; Khan et al., 2016; Morbidelli et  
299 al., 2016) and field (Sharma et al., 1983; Cerdà and García-Fayos, 1997; Chaplot and Le  
300 Bissonnais, 2000; Janeau, 2003; Ribolzi et al., 2011; Patin et al., 2012) settings. Even though  
301 these studies provided conflicting results as to whether infiltration increase or decrease with  
302 slope, all of them provided useful insights.

303

#### 304 **3.1 Laboratory simulations**

305 Useful conclusions were derived by Essig et al. (2009) and Morbidelli et al. (2015, 2016) by  
306 examining results obtained from a long series of laboratory experiments conducted with an  
307 experimental system consisting of:

- 308 – a soil box with characteristics shown in Fig. 3 and the slope adjustable in the range 1-  
309 25°;
- 310 – study soils of thickness 67 cm obtained from natural soils, over 7 cm of gravel to  
311 speed the drainage of the percolated water from the soil;

- 312 – a rainfall simulator, based on sprinklers of water under pressure provided by a pump,  
313 that produces a uniform rainfall distributed over the soil surface of intensity calibrated  
314 in advance and chosen through the appropriate combination of sprinkler type and  
315 water pressure;
- 316 – tipping bucket sensors that provided continuous surface and deep flow at the  
317 downstream soil boundary;
- 318 – time domain reflectometry sensors that collect continuous observations of the average  
319 soil water content at different depths in two vertical profiles.

320 A first set of 50 experiments was discussed by Essig et al., (2009) with three different soil  
321 types (a clay loam, a loam and a sandy loam; each soil type designation hereinafter is based  
322 on the USDA classification), slopes ranging from 1° to 15° and rainfall rates in the range 10-  
323 30 mmh<sup>-1</sup>. For each experiment, rainfall was applied to reach soil saturation throughout the  
324 box. Surface runoff and deep flow were collected for up to 24 h. It was observed that the time  
325 to ponding increased as rainfall intensities decreased. Surface flowrate (normalized by the  
326 average rainfall rate) versus time were used to compare runoff rates for different slopes, soil  
327 types, and rainfall rates. For the clay loam soil, the slope had a great positive effect on the  
328 steady state surface flow. Based on kinematic wave theory, the time of concentration should  
329 be under one hour. However, the duration of the observed receding limb of surface flow was  
330 longer than expected after the rainfall was turned off. This tail was more prominent for  
331 steeper slopes and less evident for coarse soils. The normalized infiltration rates for the clay  
332 loam soil (Essig et al., 2009) suggested the presence of soil water outflow near saturation (i.e.  
333 a seepage face), but this was not as obvious for the loam and the sandy loam soils. On the  
334 basis of the above theoretical formulations, one would expect that the normalized steady deep  
335 flow should only vary by a factor of  $\cos(\gamma)$ , but the results reported in Essig et al. (2009) did  
336 not conform to this expectation and the steady deep flow decreased by much larger amounts

337 with slope angle. Three different mathematical models were employed to explain the  
338 measured data. The authors proposed an effective saturated hydraulic conductivity, that  
339 empirically accounts for slope effects, to obtain realistic agreements with measurements of  
340 overland flow, deep flow and water content at different depths.

341

342

343 *insert here Fig. 3*

344

345

346 After an on overall analysis of the observed results, Essig et al. (2009) postulated that  
347 relationships between rainfall and surface runoff (and deep flow) were being influenced by  
348 the following aspects:

- 349 - The walls of the sand box enforced a condition of zero flux normal to the boundary.  
350 This might be altering the flow pattern sufficiently so that the flow was strongly  
351 influenced by wall effects.
- 352 - A longer recession tail, particularly for the steeper slopes in the clay loam soil  
353 suggested the existence of return flow from saturated areas. This return flow, if it  
354 exists, would be more noticeable for steep slopes and for fine-textured soils.
- 355 - The infiltration of water moving on the sloping soil surface was different from the case  
356 of infiltration over a flat surface where the ponded water had no momentum in the  
357 direction tangential to the slope.

358 To shed more light on these issues, Morbidelli et al., (2015) carried out a second set of 15  
359 laboratory experiments with two important modifications:

- 360 - surface runoff assimilation by a technique which enabled to perform measurements in  
361 the middle of the box (along the slope);

362 - much lower values of the ratio  $r/K_s$  changed from  $\sim 2-3$  to  $\sim 0.7-1.3$ .

363 The first modification allowed the authors to eliminate the effect of the downstream boundary  
364 on the separation between surface and subsurface flows. The second modification extended  
365 the investigation to commonly observed rainfall rates and assured the absence of both erosion  
366 and sealing layer.

367 Results by Morbidelli et al. (2015) indicate that, even for moderate rainfall rates, the variation  
368 of the subsurface flow with  $\gamma$  is very evident. Their results, which refer substantially to  
369 conditions with prevailing gravitational effects, do not agree with any theoretical result, and  
370 further support the trends shown by Essig et al. (2009). Morbidelli et al. (2015) suggested the  
371 existence of a relation between the decrease of the steady deep flow with  $\gamma$  and the shear  
372 stress at the soil surface as a basis for estimating an effective saturated hydraulic conductivity  
373 to be used in the existing infiltration models for horizontal surfaces. In this context, the role of  
374 the surface roughness remained an open problem to be addressed through specific field and  
375 laboratory experiments. Furthermore, for bare sloping surfaces Morbidelli et al. (2015) noted  
376 the production of surface runoff even for  $r < K_s$

377 In a subsequent set of laboratory experiments, Morbidelli et al. (2016) provided experimental  
378 evidence on the role of roughness in the relation between infiltration and slope angle. Twenty-  
379 eight new simulations were performed by the same experimental system but using a grassy  
380 soil surface. Morbidelli et al. (2016) provided fresh evidence of the relationship between  $\gamma$   
381 and infiltration rate on a grassy soil and remarked the significant differences existing between  
382 bare and grassy soils. Their laboratory simulations highlighted that the effect of slope gradient  
383 on infiltration rate was greatly reduced by the grassy soil surface with a smaller decrease of  
384 the steady infiltration rate for  $\gamma$  in the range  $1-15^\circ$ . More specifically, their results provided  
385 evidence of the existence of an effective soil saturated hydraulic conductivity,  $K_e(\gamma)$ ,  
386 associated with rainfall rates that yielded surface runoff and steady deep flow for each  $\gamma$



387 value. This quantity decreased from  $\sim K_s$  for  $\gamma=1^\circ$  down to  $\sim 0.8 K_s$  for  $\gamma=10^\circ$ . The divergence  
388 with results computed by theoretical formulations is much more significant in the case of a  
389 bare soil for which, from Morbidelli et al. (2015),  $K_e(\gamma=10^\circ)\approx 0.2 K_s$ . A common feature of  
390 slopes with grassy soils and bare soils concerns the production of surface runoff for  $K_e < r < K_s$ ,  
391 that is in unsaturated soils. Furthermore: (1) the trials presented in the work for a grassy soil  
392 by Morbidelli et al. (2016) coupled with those earlier described for bare soils by Essig et al.  
393 (2009) and Morbidelli et al. (2015) suggest that the magnitude of the effects of  $\gamma$  on the  
394 gravitational component of infiltration rate is determined by a mechanism independent of the  
395 formation of rills or a sealing layer. In fact the experiments were not affected by the last two  
396 processes, which influenced several previous investigations; (2) the formation of a two-  
397 layered soil due to the grass growth cannot describe the effects of  $\gamma$  on the infiltration rate;  
398 and (3) the relation between  $\gamma$  and infiltration rate is strictly dependent on the surface  
399 roughness.

400 Along the same lines, Nassif and Wilson (1975), Fox et al. (1997), Mu et al. (2015) and Khan  
401 et al. (2016) conducted laboratory experiments and found that the infiltration rate decreased  
402 with increasing slope angle. Nassif and Wilson (1975) used a laboratory apparatus of  
403 horizontal dimensions 6.15 x 4.10 m and soil depth 0.22 m and an artificial rainfall generator  
404 to collect data about runoff and infiltration in different soil types and for different surface  
405 slopes. Among other results, they emphasized that the increase of slope had little effect on  
406 runoff in relatively impermeable soils and significant effects on natural soils, with an  
407 increase up to 16% and 24% in bare and grassed surfaces, respectively. They also observed a  
408 critical slope over which the peak runoff became invariant.

409 Fox et al. (1997) used a sandy loam soil, susceptible to surface crusting (Fox, 1994), packed  
410 in a 100 x 40 x 10 cm trays by applying successive layers with light compaction and  
411 smoothing between layers. The trays were set at different slope angles in the range 1.5-21.5°,

412 subjected to rainfall rate in the range 38.2-56.3 mmh<sup>-1</sup>, each with duration of 90 minutes.  
413 Infiltration was calculated from the overland flow rate, and microtensiometers and  
414 micromorphological analysis were used to characterize seal formation. Infiltration rate  
415 decreased with increasing slope angle until 11.5° and remained unchanged at steeper slope  
416 angles. The image analysis of pore characteristics clearly suggested that the slope angle had  
417 no significant impact on surface seal development. The estimated change in mean overland  
418 flow depth with slope angle was in the order of about 1 mm, and from visual observations it  
419 never appeared to exceed a few mm within any flow thread. In the presence of a sub-seal  
420 pressure head from about -100 mm to -200 mm, an additional positive pressure head at the  
421 surface of 1 mm is insignificant and in itself would not increase the infiltration rate. So the  
422 change in overland flow depth did not add sufficient pressure head to account for the change  
423 in observed infiltration rate. However, the increase in depth would be sufficient to submerge  
424 significant portions of the high locations of the microtopography. Hence, small changes in  
425 flow depth may increase the infiltration rate by submerging areas of slightly greater hydraulic  
426 conductivity around the more stable aggregates.

427 Mu et al. (2015) conducted laboratory simulations to study the effects of various factors  
428 including the slope gradient on the runoff generation mechanism in a soil cultivated with  
429 spring maize during three growing stages (jointing stage, tasseling stage and mature stage).  
430 They selected a sandy loam soil packed in a 200 x 50 x 60 cm steel bin, with slope variable in  
431 the range 0°-30°. Through some experimental trials with different combinations of rainfall  
432 intensity, slope gradient, and growing phase, they found that the overland flow and the  
433 cumulative runoff increased with the increase of rainfall rate and slope in each vegetation  
434 stage. Within a single growing stage of spring maize, they found that the runoff coefficient  
435 increased with increasing slope because of to a decrease in the soil infiltration rate, and  
436 proposed an empirical relationship that provides the runoff coefficient by a logarithmic

437 dependency on the sine of slope. Largest runoff coefficients were found for the mature stage  
438 with values increasing from 0.22 to 0.41 for slopes changing from 5° to 20° under a rainfall  
439 rate of 0.5 mm/min.

440 Khan et al. (2016) adopted an artificial rainfall generator with 324 nozzles and runoff trays  
441 that could be adjusted to the desired slope angle in the range 5°-25°. They conducted 72  
442 simulation runs under numerous combinations both in mulched and un-mulched silty loam  
443 soils with rainfall intensities ranging between 33 mmh<sup>-1</sup> and 120 mmh<sup>-1</sup>. The duration for each  
444 rainfall event was 1 h and steady conditions were never reached. Khan et al. (2016) found that  
445 infiltration rate decreased with an increase in slope and increased with an increase in rainfall  
446 intensity. They concluded that the effect of rainfall intensity on the infiltration rate changed  
447 with the slope angle due to the creation of different micro-relief features and that in mulched  
448 soil the water infiltration rate significantly increased with an increase in rainfall intensity at all  
449 slope angles because of the uniform surface conditions under the mulch layers. These trends  
450 agreed with those showed by Essig et al. (2009) and Morbidelli et al. (2015, 2016), with the  
451 magnitudes of the reduction in infiltration with slope much larger than expected from all  
452 theoretical studies.

453 On the other hand, Poesen (1984) found that the infiltration rate increased with increasing  
454 slope angle. In fact, his experimental results were characterized by a decrease in runoff with  
455 increasing slope for soils subjected to surface crust formation. Specifically, the runoff  
456 coefficient was found to be higher for a 2% slope than a 15% slope, and the mean percolation  
457 coefficient was lower for the 2% than 15% slope. These results, incidentally very similar to  
458 results by Assouline and Ben-Hur (2006), indicated a positive relationship between slope and  
459 infiltration rate, which was more pronounced for soils with water content at field capacity or  
460 greater. Poesen (1984) attributed the decreased runoff to either a thinner soil crust or  
461 increased rill erosion on the steeper slopes and concluded that 1) surface sealing is inversely

462 related to slope, so steeper slopes would have a thinner compressed soil layer than flatter  
463 slopes and would be more prone to infiltration, 2) steeper slopes erode more quickly and  
464 increased erosion forms deeper rills, thus the surface area over which infiltration can occur  
465 becomes larger, and 3) in the absence of erosion and surface sealing the slope would not be  
466 expected to affect the infiltration process.

467 Of particular interest are also the analyses conducted to clarify the effect of different slope  
468 angles on water movement during unsaturated stages. For example, laboratory experiments  
469 were carried out by Lv et al. (2013) considering the redistribution process in a variable-slope  
470 soil tank (from 0° to 30°), with a homogeneous and isotropic sandy loam soil. The results  
471 showed that, increasing the slope became larger the gradient of soil water potential in the  
472 lateral downslope direction parallel to the slope surface. It was concluded that the water  
473 movement in the lateral downslope direction parallel to the slope surface was more sensitive  
474 to changes in the slope angle than the component normal to the slope surface. Lv et al. (2013)  
475 also observed that the influence of the slope angle on the flow component normal to the slope  
476 surface was greatest at a certain depth into the soil .

477

### 478 3.2 Field experiments

479 With the main objective to analyze the effect of slope angle on interrill erosion for different  
480 plot sizes and to identify possible detachment and transport processes involved in the relations  
481 between slope, rain characteristics and plot sizes, Chaplot and Le Bissonnais (2000)  
482 conducted a detailed study in an experimental field located in the northwest part of the Paris  
483 basin. The site was characterized by silty loam soils very susceptible to soil crusting. The  
484 experimental field was about 100 m in length and located in the middle of a convexo-concave  
485 catena with slope gradients of about 2%, 4%, 8% and 2% from top to bottom. Three 1 x 1 m  
486 bounded plots were established at three positions along the catena with slopes 2%, 4% and

487 8%. Two additional 2 x 5 m bounded plots were selected at the 4% and 8% slope positions.  
488 Six natural rainfall events (total rainfall depth of about 100 mm, intensities in the range 1.31-  
489 8.00 mmh<sup>-1</sup>), in addition to artificial rainfalls with intensities up to 50 mmh<sup>-1</sup>, were  
490 considered. Flow depth and detention capacity were very low because of initially smooth  
491 crusted surfaces. Infiltration rates were computed from runoff rates and rainfall intensity. As  
492 slope increased from 2% to 8%, infiltration decreased from 1 to 0.5 mmh<sup>-1</sup> for low intensity  
493 natural rains, from 4 to 1 mmh<sup>-1</sup> for 8 mmh<sup>-1</sup> natural rain, and from 15 to 5 mmh<sup>-1</sup> for 50  
494 mmh<sup>-1</sup> artificial rainfall. Increase in flow velocity with slope steepness and length was  
495 considered to be a possible explanation of the slope effect on runoff. No rills occurred in this  
496 study. The slope effect on runoff was substantially the same for both the 10 m<sup>2</sup> and 1 m<sup>2</sup> plots.  
497 Scale effect on runoff does not seem to be important for the range of scales adopted.  
498 Earlier, Sharma et al. (1983) had conducted field experiments for a period of six years on a  
499 representative loamy sand soil. Plots with slopes ranging from 0.5% to 10% and slope lengths  
500 ranging from 5.12 m to- 14.5 m were used. Under natural rainfall depths, they found that with  
501 dry antecedent soil conditions infiltration was governed by rainfall depth, whereas with wet  
502 antecedent soil conditions raindrop impact which formed a crust over the soil surface was the  
503 deciding factor. Infiltration decreased significantly with increasing slope due to reduction in  
504 the time available for rainfall to infiltrate, but a slope length had no substantial effect.  
505 Opposite conclusions were reached by Janeau et al. (2003) about infiltrability and slope  
506 gradient under field conditions through experiments on a gravelly loamy soil occupying the  
507 upper half of a cultivated convex hill in northern Thailand. Fifteen 1 x 1 m plots with slope  
508 gradients in the range 16-63% were selected, and different artificial rainfall patterns were  
509 chosen. The steady final infiltration rate increased sharply with increasing slope gradient.  
510 Microaggregates tended to behave like sand and became tightly packed on moderate slopes  
511 (packing crust). From these results Janeau et al. (2003) deduced that the vertical component of

512 kinetic energy (greater on moderate slope) had a prevailing role. Furthermore they asserted  
513 that 1) on steep slopes the horizontal component of the kinetic energy was transformed into  
514 shear stress, impeding the development of crusts so that water could still infiltrate, and 2) on  
515 steeper slopes, the water film was thinner, thereby limiting the role of splash. Janeau et al.  
516 (2003) concluded that the relationship between slope gradient and infiltrability is affected by  
517 the soil nature and should be investigated considering surface crusting processes.

518 Infiltration experiments conducted by Ribolzi et al. (2011) in two small plots characterized by  
519 very different slopes with rainfall intensities in the range 60-120 mmh<sup>-1</sup> produced results  
520 similar to that previously described (Janeau et al., 2003); final infiltration rates of 6 mmh<sup>-1</sup>  
521 and 21 mmh<sup>-1</sup> were obtained for the 30% and 75% slopes, respectively. These experiments  
522 confirm the hypothesis that higher effective rainfall intensity is responsible for the  
523 development of less permeable erosion crust under low slope gradients whereas more  
524 permeable structural crust develop under high slope gradients.

525 Finally, during a long-term survey of a small agricultural basin in Lao, Patin et al. (2012)  
526 achieved interesting results as part of analyses of surface runoff formation at plot scale. They  
527 observed that infiltrability decreased when slope increased up to approximately 50% and  
528 increased with slope for steeper slopes (>50%), probably due to two opposite trends: when the  
529 soil is covered, at least partly, with vegetation, crust cover remains limited and infiltration can  
530 decrease normally with increasing slope. When the soil is bare, as commonly observed for  
531 steep slope, the opposed relationship is achieved due to lesser development of crust.

532

#### 533 **4. Assessment and Future Developments**

534 Table 1 provides a summary of the experimental work dealing with infiltration on sloping  
535 surfaces and includes efforts on theoretical (conceptual) analyses along with experiments  
536 carried out in both laboratory and field settings. This article suggests that the interaction

537 between surface and subsurface waters seems to be more nuanced than would be suggested by  
538 our current understanding of infiltration processes. The role of slope on infiltration is  
539 complicated by many confounding factors such as rainfall (or applied water) intensity,  
540 microtopography, vegetation, soil texture, and vertical and horizontal heterogeneity in soil  
541 properties. Consequently, the conclusions from previous studies have been mixed and even  
542 contradictory, perhaps because the results of the experiments studying the role of slope on  
543 infiltration were also influenced by one or more of these confounding factors in different  
544 ways.

545 There is growing laboratory evidence that the reduction in infiltration occurs beyond the  $\cos \gamma$   
546 factor expected during steady saturated conditions. This is especially prominent for  
547 infiltration over bare slopes and for clay soils, and becomes less prominent for vegetated  
548 surfaces and sandy soils. When studies have reported an apparent increase in infiltration, this  
549 has perhaps been due to the formation of a sealing layer, or because of some complications  
550 introduced through rill formation. Experiments that were designed to eliminate these effects  
551 have reinforced this behavior of increased infiltration beyond what is expected from a cosine  
552 of the slope angle. The number of repeated (and repeatable) experiments from multiple  
553 research groups, suggests that this trend is not merely measurement error or experimental  
554 aberration, and warrants careful scrutiny.

555 The development and testing of new theoretical underpinnings for to describe infiltration on  
556 sloping surfaces is needed to move the science forward. While researchers have postulated  
557 that tangential velocities at the soil surface, the increased depth of water in microtopographic  
558 depressions, or shear stress exerted by the overland water on the soil surface might cause this  
559 apparent increase in infiltration rates, a comprehensive theory is still lacking. Studies have  
560 suggested the idea of an “effective saturated hydraulic conductivity” to offer an empirical  
561 correction, but have not offered a theoretical basis that would allow this understanding to be

562 extended to other cases beyond those covered by the range of experiments. A physical  
563 explanation followed by supporting mathematical formulation would be an important step in  
564 either supporting the hypothesis of increased infiltration with slope, or provide refutation of  
565 this notion and provide an explanation for the experimental results that support this  
566 hypothesis. Such a theory would also serve to inform us as to what future experiments to  
567 conduct and what to measure to close the gaps in our understanding.

568 Researchers conducting field-scale experiments have to contend with the natural spatial  
569 variability in hydraulic properties of soils and the associated role of run-on. Experimental  
570 efforts often measure averaged quantities such as rainfall and runoff from the entire field, i.e.  
571 integrated responses. As was noted earlier, it is very difficult to make independent point-scale  
572 measurements at all space and time scales, and therefore need both a good local model as  
573 noted in the previous paragraph, and a description of the nature of the spatial variation of  
574 hydraulic properties to perform upscaling studies.

575 Extensions of infiltration models to watershed scales are, of course, further complicated with  
576 variability at more spatial scales and the role of channel networks, and current practice relies  
577 on calibration and corroboration approaches at these scales. This operational process will  
578 have to be the state of practice until a meaningful way of upscaling knowledge from sub-grid  
579 scales is developed.

580

581

582 *insert here Tab. 1*

583

584



585 **Acknowledgment**

586 This research was mainly financed by the Italian Ministry of Education, University and  
587 Research (PRIN 2015).

588

589

590 **References**

591 Assouline, S., Ben-Hur, M., 2006. Effects of rainfall intensity and slope gradient on the  
592 dynamics of interrill erosion during soil surface sealing. *Catena* 66(3), 211-220.

593 Beven, K.J., 2002. *Rainfall-Runoff Modelling*, Wiley.

594 Broadbridge, P., White, I., 1988. Constant rate rainfall infiltration: A versatile nonlinear  
595 model. 1, Analytic solution. *Water Resour. Res.* 24, 145-154.

596 Bronstert, A., Bardossy, A., 1999. The role of spatial variability of soil moisture for modeling  
597 surface runoff generation at the small catchment scale. *Hydrol. Earth Syst. Sc.* 3, 505-516.

598 Castelli, F., 1996. A simplified stochastic model for infiltration into a heterogeneous soil  
599 forced by random precipitation. *Adv. Water Resour.* 19(3), 133-144.

600 Cerdà, A., García-Fayos, P., 1997. The influence of slope angle on sediment, water and seed  
601 losses on badland landscapes. *Geomorphology* 18(2), 77-90.

602 Chaplot, V., Le Bissonais, Y., 2000. Field measurements of interrill erosion under different  
603 slopes and plot sizes. *Earth Surf. Process. Landforms* 25, 145-153.

604 Chen, L., Young, M.H., 2006. Green-Ampt Infiltration Model for Sloping Surfaces. *Water*  
605 *Resour. Res.* 42, W07420.

606 Chow, V.T., Maidment, D.R., Mays, L.W., 1988. *Applied Hydrology*, McGraw-Hill, New  
607 York.

608 Chu, S.T., 1978. Infiltration during an unsteady rain. *Water Resour. Res.* 14(3), 461-466.

609 Corradini, C., Melone, F., Smith, R.E., 1994. Modeling infiltration during complex rainfall  
610 sequences. *Water Resour. Res.* 30(10), 2777-2784.

611 Corradini, C., Melone, F., Smith, R.E., 1997. A unified model for infiltration and  
612 redistribution during complex rainfall patterns. *J. Hydrol.* 192, 104-124.

613 Corradini, C., Melone, F., Smith, R.E., 2000. Modeling local infiltration for a two layered soil  
614 under complex rainfall patterns. *J. Hydrol.* 237, 58-73.

615 Corradini, C., Flammini, A., Morbidelli, R., Govindaraju, R.S., 2011. A conceptual model for  
616 infiltration in two-layered soils with a more permeable upper layer: From local to field  
617 scale. *J. Hydrol.* 410, 62-72.

618 Dagan, G., Bresler, E., 1983. Unsaturated flow in spatially variable fields, 1, Derivation of  
619 models of infiltration and redistribution. *Water Resour. Res.* 19(2), 413-420.

620 Essig, E.T., Corradini C., Morbidelli, R., Govindaraju, R.S., 2009. Infiltration and deep flow  
621 over sloping surfaces: Comparison of numerical and experimental results. *J. Hydrol.* 374,  
622 30-42.

623 Fiori, A., Romanelli, M., Cavalli, D.J., Russo, D., 2007. Numerical experiments of  
624 streamflow generation in steep catchments. *J. Hydrol.* 339, 183-192.

625 Fox, D.M., Bryan, R.B., Price, A.G., 1997. The influence of slope angle on final infiltration  
626 rate for interrill conditions. *Geoderma* 80, 181-194.

627 Govindaraju, R.S., Corradini, C., Morbidelli, R., 2006. A semi-analytical model of expected  
628 areal-average infiltration under spatial heterogeneity of rainfall and soil saturated hydraulic  
629 conductivity. *J. Hydrol.* 316, 184-194.

630 Govindaraju, R.S., Morbidelli, R., Corradini, C., 2001. Areal infiltration modelling over soils  
631 with spatially correlated hydraulic conductivities. *J. Hydrol. Eng.* 6(2), 150-158.

632 Govindaraju, R. S., Corradini, C., Morbidelli, R., 2012. Local and field-scale infiltration into  
633 vertically non-uniform soils with spatially-variable surface hydraulic conductivities.  
634 *Hydrol. Proc.* 26 (21), 3293-3301.

635 Green, W.A., Ampt, G.A., 1911. Studies on soil physics: 1. The flow of air and water through  
636 soils. *J. Agricol. Sci.* 4, 1-24.

637 Greminger P.J., Sud, Y.K., Nielsen, D.R., 1985. Spatial variability of field measured soil-  
638 water characteristics. *Soil Sci. Soc. Am. J.* 49(5), 1075-1082.

639 Holtan, H.N., 1961. A concept for infiltration estimates in watershed engineering. *USDA*  
640 *Bull.*, 41-51.

641 Horton, R.E., 1940. An approach toward a physical interpretation of infiltration-capacity. *Soil*  
642 *Sci. Soc. Am. J.* 5, 399-417.

643 Hu, W., She, D., Shao, M., Chun, K.P., Si, B., 2015. Effects of initial soil water content and  
644 saturated hydraulic conductivity variability on small watershed runoff simulation using  
645 LISEM. *Hydrol. Sci. J.* 60(6), 1137-1154.

646 Janeau, J.L., Bricquet, J.P., Planchon, O., Valentin, C., 2003. Soil crusting and infiltration on  
647 steep slopes in northern Thailand. *Europ. J. Soil Sci.* 54, 543-553.

648 Khan, M.N., Gong, Y., Hu, T., Lal, R., Zheng, J., Justine, M.F., Azhar, M., Che, M., Zhang,  
649 H., 2016. Effect of slope, rainfall intensity and mulch on erosion and infiltration under  
650 simulated rain on purple soil of south-western Sichuan province, China. *Water* 8(11), 528.

651 Kostiakov, A.N., 1932. On the dynamics of the coefficient of water-percolation in soils and  
652 on the necessity for studying it from a dynamic point of view for purposes of amelioration.  
653 *Trans. Sixth Comm. Intern. Soil Sci. Soc. Russian, part A*, 17-21.

654 Loague, K., Gander, G.A., 1990. R-5 revisited, 1, Spatial variability of infiltration on a small  
655 rangeland catchment. *Water Resour. Res.* 26(5), 957-971.

656 Lv, M., Hao, Z., Liu, Z., Yu, Z., 2013. Conditions for lateral downslope unsaturated flow and  
657 effects of slope angle on soil moisture movement. *J. Hydrol.* 486, 321-333.

658 Mein, R.G., Larson, C.L., 1973. Modeling infiltration during a steady rain. *Water Resour.*  
659 *Res.* 9, 384-394.

660 Mls, J., 1980. Effective rainfall estimation. *J. Hydrol.* 45, 305-311.

661 Morbidelli, R., Corradini, C., Govindaraju, R.S., 2006. A field-scale infiltration model  
662 accounting for spatial heterogeneity of rainfall and soil saturated hydraulic conductivity.  
663 *Hydrol. Proc.* 20, 1465-1481.

664 Morbidelli, R., Corradini, C., Saltalippi, C., Brocca, L., 2012. Initial soil water content as  
665 input to field-scale infiltration and surface runoff models. *Water Resour. Manag.* 26, 1793-  
666 1807.

667 Morbidelli, R., Saltalippi, C., Flammini, A., Cifrodelli, M., Corradini, C., Govindaraju, R.S.,  
668 2015. Infiltration on sloping surfaces: Laboratory experimental evidence and implications  
669 for infiltration modelling. *J. Hydrol.* 523, 79-85.

670 Morbidelli, R., Saltalippi, C., Flammini, A., Cifrodelli, M., Picciafuoco, T., Corradini, C.,  
671 Govindaraju, R.S., 2016. Laboratory investigation on the role of slope on infiltration over  
672 grassy soils. *J. Hydrol.* 543, 542-547.

673 Mu, W., Yu, F., Li, C., Xie, Y., Tian, J., Liu, J., Zhao, N., 2015. Effects of rainfall intensity  
674 and slope gradient on runoff and soil moisture content on different growing stages of  
675 spring maize. *Water* 7, 2990-3008.

676 Mualem, Y., Assouline, S., Eltahan, D., 1993. Effect of rainfall-induced soil seals on soil  
677 water regime: Wetting processes. *Water Resour. Res.* 29(6), 1651-1659.

678 Nassif, S.H., Wilson, E.M., 1975. The influence of slope and rain intensity on runoff and  
679 infiltration. *Hydrol. Sci. Bull.* 20(4), 539-553.

680 Nielsen D.R., Biggar, J.W., Erh, K.T., 1973. Spatial variability of field measured soil-water  
681 properties. *Hilgardia* 42(7), 215-259.

682 Parlange J.-Y., Lisle, I., Braddock, R.D., Smith, R.E., 1982. The three-parameter infiltration  
683 equation. *Soil Sci.* 133(6), 337-341.

684 Patin, J., Mouche, E., Ribolzi, O., Chaplot, V., Sengtaheuanghoung, O., Latsachak, K.O.,  
685 Soulileuth, B., Valentin, C., 2012. Analysis of runoff production at the plot scale during a  
686 long-term survey of a small agricultural catchment in Lao PDR, *J. Hydrol.* 426-427, 79-92.

687 Péschke, G., Kutílek, M., 1982. Infiltration model in simulated hydrographs. *J. Hydrol.* 56,  
688 369-379.

689 Philip, J.R., 1957a. The theory of infiltration: 1. The infiltration equation and its solution. *Soil*  
690 *Sci.* 83, 345-357.

691 Philip, J.R., 1957b. The theory of infiltration: 2. The profile at infinity. *Soil Sci.* 83, 435-448.

692 Philip, J.R., 1957c. The theory of infiltration: 4. Sorptivity algebraic infiltration equation. *Soil*  
693 *Sci.* 84, 257-264.

694 Philip, J.R., 1991. Hillslope Infiltration: Planar Slopes. *Water Resour. Res.* 27(1), 109-117

695 Poesen, J., 1984. The Influence of Slope Angle on Infiltration Rate and Hortonian Overland  
696 Flow Volume. *Z. Geomorphol.* 49, 117-131.

697 Reeves, M., Miller, E.E., 1975. Estimating infiltration for errating rainfall. *Water Resour.*  
698 *Res.* 11(1), 102-110.

699 Ribolzi, O., Patin, J., Bresson, L., Latsachack, K., Mouche, E., Sengtaheuanghoung, O.,  
700 Silvera, N., Thiébaux, J.P., Valentin, C., 2011. Impacy of slope gradient on soil surface  
701 features and infiltration on steep slopes in northern Laos. *Geomorphology* 127(1-2), 53-63.

702 Russo, D., Bresler, E., 1981. Soil hydraulic properties as stochastic processes, 1, Analysis of  
703 field spatial variability. *Soil Sci. Soc. Am. J.* 45, 682-687.

704 Russo, D., Bresler, E., 1982. A univariate versus a multivariate parameter distribution in a  
705 stochastic-conceptual analysis of unsaturated flow. *Water Resour. Res.* 18(3), 483-488.

706 Sharma, K., Singh, H., Pareek, O., 1983. Rain water infiltration into a bar loamy sand.  
707 *Hydrol. Sci. J.* 28, 417-424.

708 Sharma, M.L., Barron, R.J.W., Fernie, M.S., 1987. Areal distribution of infiltration  
709 parameters and some soil physical properties in lateritic catchments. *J. Hydrol.* 94, 109-  
710 127.

711 Sivapalan, M., Milly, P.C.D., 1989. On the relationship between the time condensation  
712 approximation and the flux concentration relation. *J. Hydrol.* 105(3-4), 357-367.

713 Smith, R.E., Corradini, C., Melone, F., 1993. Modeling infiltration for multistorm runoff  
714 events. *Water Resour. Res.* 29(1), 133-144.

715 Smith, R.E., Corradini, C., Melone, F., 1999. A conceptual model for infiltration and  
716 redistribution in crusted soils. *Water Resour. Res.* 35(5), 1385-1393.

717 Smith, R.E., Goodrich, D.C., 2000. A model to simulate rainfall excess patterns on randomly  
718 heterogeneous areas. *J. Hydrol. Eng.* 5(4), 355-362.

719 Smith, R.E., Parlange, J.-Y., 1978. A parameter-efficient hydrologic infiltration model. *Water*  
720 *Resour. Res.* 14, 533-538.

721 Soil Conservation Service, 1972. *SCS National Engineering Handbook, Sec. 4, Hydrology,*  
722 *USDA.*

723 Swartzendruber, D., 1987. A quasi solution of Richard equation for downward infiltration of  
724 water into soil. *Water Resour. Res.* 5, 809-817.

725 Taha, A., Gresillon, J.M, Clothier, B.E., 1997. Modelling the link between hillslope water  
726 movement and stream flow: application to a small Mediterranean forest watershed. *J.*  
727 *Hydrol.* 203, 11-20.

728 Verma, S.C., 1982. Modified Horton's infiltration equation. *J. Hydrol.* 58, 383-388.

729 Wang, J., Chen, L., Yu, Z., 2018. Modeling rainfall infiltration on hillslopes using flux-  
730 concentration relation and time compression approximation. *J. Hydrol.* 557, 243-253.

731 Warrick, A.W., Nielsen, D.R., 1980. Spatial variability of soil physical properties in the field.  
732 In: D. Hillel (Editor), *Applications of Soil Physics*. Academic Press, New York, New  
733 York, 319-344.

734 Wood, E.F., Sivapalan, M., Beven, K., 1986. Scale effects in infiltration and runoff  
735 production. *Proc. of the Symposium on Conjunctive Water Use*, IAHS Publ. N. 156,  
736 Budapest.

737

738

739

740

741

742

743

744

745

746

747 **List of Tables**

748

749 **Table 1** – Main characteristics of scientific studies analyzing the role of slope on infiltration.

750

751

752

753

754

755

756 **Figure captions**

757

758 **Fig. 1** – Cartesian spatial coordinates with schematic representation of flow velocities normal  
759 to the slope,  $v_n$ , and in vertical direction,  $v$ .

760

761 **Fig. 2** –Representation of the step function of soil moisture profile for sloping surface. For  
762 symbols see text.

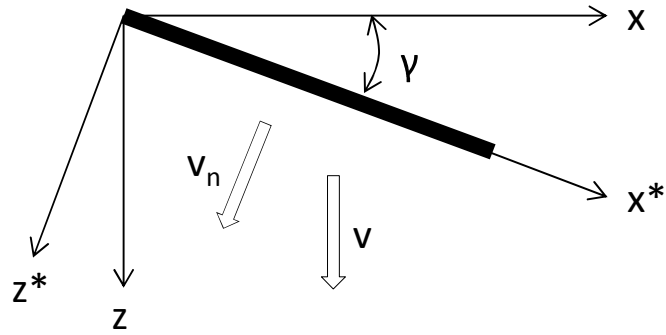
763

764 **Fig. 3** – Schematic representation of the laboratory system with variable slope angle adopted  
765 by Essig et al. (2009), and Morbidelli et al. (2015; 2016).

766

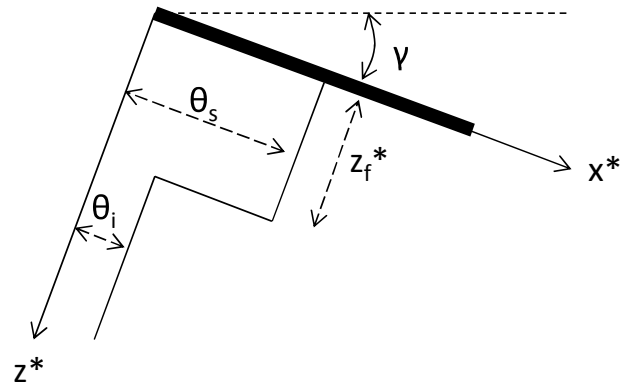


Figure 1



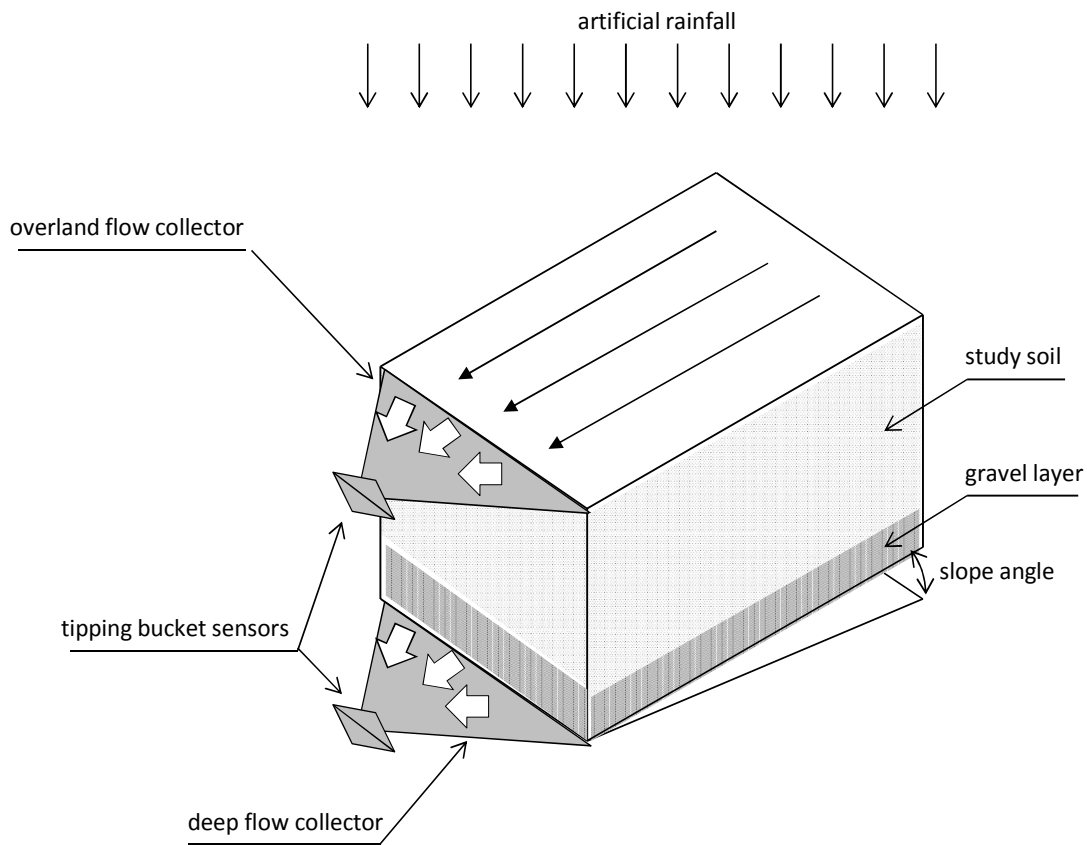
**Fig. 1** – Cartesian spatial coordinates with schematic representation of flow velocities normal to the slope,  $v_n$ , and in vertical direction,  $v$ .

Figure 2



**Fig. 2** – Representation of the step function of soil moisture profile for sloping surface. For symbols see text.

**Figure 3**



**Fig. 3** – Schematic representation of the laboratory system with variable slope angle adopted by Essig et al. (2009), and Morbidelli et al. (2015; 2016).

**Table 1** – Main characteristics of scientific studies analyzing the role of slope on infiltration

<b>Authors</b>	<b>Year</b>	<b>Analysis type</b>	<b>Soil type</b>	<b>Slope range</b>	<b>Main insight</b>
<i>Nassif and Wilson</i>	1975	experimental (laboratory)	sandy clay, peat, standard agricultural soil	0%-32%	vertical infiltration decrease with increasing slope (it exists a critical slope beyond which infiltration remain unchanged)
<i>Sharma et al.</i>	1983	experimental (field)	loamy sand	0.5% - 10%	vertical infiltration decrease with increasing slope (less time for rainfall to infiltrate)
<i>Poesen</i>	1984	experimental (laboratory)	sandy, silty	2° - 20°	vertical infiltration increase with increasing slope (thinner crust and more rill erosion)
<i>Philip</i>	1991	theoretical (analytical)	-	-	normal infiltration decrease with increasing slope (by a factor $\cos(\gamma)$ )
<i>Cerdà and García-Fayos</i>	1997	experimental (field)	loam, silty-loam, silty-clay, silty clay-loam	2° - 55°	vertical infiltration independent by slope angle
<i>Fox et al.</i>	1997	experimental (laboratory)	sandy loam	1.5° - 21.5°	vertical infiltration decrease with increasing slope until $\sim 11^\circ$ (interaction between flow depth and submerged areas)
<i>Chaplot and Le Bissonnais</i>	2000	experimental (field)	silty loam	2% - 8%	vertical infiltration significantly decrease with increasing slope (increase of flow velocity with slope steepness)
<i>Janeau et al.</i>	2003	experimental (field)	loamy	16% - 63%	vertical infiltration increase with increasing slope (the vertical component of kinetic energy has a dominant role)
<i>Assouline and Ben-Hur</i>	2006	experimental (laboratory)	sandy	5° - 25°	vertical infiltration increase with increasing slope (thinner crust and more rill erosion)
<i>Chen and Young</i>	2006	theoretical (conceptual)	-	-	normal infiltration increase (by $\cos(\gamma)$ ) with increasing slope (only a $t \rightarrow 0$ and for equal horizontal projection length)

<i>Essig et al.</i>	2009	experimental (laboratory)	clay loam, loam, sandy loam	1° - 15°	vertical infiltration decrease with increasing slope (for the presence of return flow from saturated areas)
<i>Ribolzi et al.</i>	2011	experimental (field)	clay loam	30% - 70%	vertical infiltration increase with increasing slope (a more permeable structural crust develop under steep slopes)
<i>Patin et al.</i>	2012	experimental (field)	Entisol, Ultisol, Alfisol (US Taxonomy soil classification system)	10% - 110%	vertical infiltration decrease with increasing (up to 50%) slope and increase for steeper slopes (due to effect of crust formation and different land use)
<i>Lv et al.</i>	2013	experimental (laboratory)	sandy loam	0° - 30°	the component of flow parallel to the surface increase with slope more than the normal component
<i>Morbidelli et al.</i>	2015	experimental (laboratory)	loam	1° - 10°	vertical infiltration decrease with increasing slope (link between this decrease and shear stress at soil surface)
<i>Mu et al.</i>	2015	experimental (laboratory)	sandy loam	0° - 30°	vertical infiltration decrease with increasing slope (the surface roughness influence the slope effect)
<i>Khan et al.</i>	2016	experimental (laboratory)	silty loam	5° - 25°	vertical infiltration decrease with increasing slope (large effect of micro-relief features and rainfall intensity)
<i>Morbidelli et al.</i>	2016	experimental (laboratory)	loam (grassy)	1° - 15°	vertical infiltration decrease with increasing slope (the high surface roughness reduce the slope effect)
<i>Wang et al.</i>	2018	theoretical (conceptual)	-	-	vertical infiltration decrease with increasing slope (due to a ponding time prediction with a time compression approximation)

---